PANI-ZnO-PAN Composite Fibers for Room Temperature Ammonia Gas Sensing

Altay Ayan

Under the direction of

Dr. Almagul Mentbayeva
Assistant Professor
Nazarbayev University,
School of Engineering and Digital Sciences,
Department of Chemical and Materials Engineering

Research Orda Kazakhstan
August 8, 2025

Abstract

Ammonia (NH) is a hazardous gas commonly released from industrial processes, which requires efficient detection systems for environmental monitoring and public safety. In this study, novel PANI–ZnO–PAN composite nanofibers were fabricated for room-temperature NH3 detection. ZnO nanoparticles were synthesized via the sol–gel method, incorporated into polyacrylonitrile (PAN) solution, and electrospun into composite fibers, followed by in situ polyaniline (PANI) coating to enhance active sites and electrical conductivity. Structural and morphological analyses using XRD, SEM, TEM, and EDS confirmed the wurtzite ZnO phase, uniform fiber networks, and effective nanoparticle integration. FTIR spectroscopy verified the presence of Zn-O, PANI and PAN characteristic bonds, while UV-vis diffuse reflectance spectroscopy revealed a reduced band gap of 2.037 eV, indicating a synergistic electronic interaction between ZnO and PANI. The high surface area, porous morphology, and p-n heterojunction structure of the composite are expected to improve NH3 adsorption and charge transfer, allowing for sensitive detection under ambient conditions. This work provides a promising platform for low-cost, flexible, and high-performance gas sensors, with potential for further optimization of nanostructure uniformity, stability, and selectivity.

1 Introduction

Extreme air pollution is a pressing issue globally, as a result of rapid industrialization and urbanization. Notably, ammonia (NH_3) is one of the major toxic pollutants used in the chemical, food, fertilization, and refrigeration industries. According to the Occupational Safety and Health Administration (OSHA), the exposure limit of NH_3 to humans is 25ppm for 8 hours and 35ppm for 10 minutes; otherwise, it causes irritation of human respiratory system, skin and eyes (1). The production of fertilizers and the combustion of chemical industries emit a significant amounts of NH_3 into the environment (2). In order to examine and detect harmful gases, maintain public safety, evaluate air quality and environmental pollution (3), and stop food from spoiling (4), gas sensors are crucial. Due to their low cost, ease of manufacture (3,5), and compact size, as well as their sensitivity to gases (3), resistive gas sensors have attracted a lot of attention. The metal oxide semiconductor (MOS) sensor is particularly noteworthy. Due to the influence of crystal facets with increased surface reactivity, nanostructured MOS materials in gas sensors provide a number of benefits, including a high specific surface area and more surface active sites (6).

Among MOS materials, n-type zinc oxide (ZnO) has received attention in recent years due to a band gap of 3.37 eV and a large exciton binding energy of 60 meV (7). The ZnO-based gas sensors are the significant focus of the gas sensor research due to their excellent sensing response, good selectivity, easy fabrication, low cost, good thermal and chemical stability, and non-toxicity(7). Despite many research efforts on utilizing ZnO sensing material for NH3 detection, there remains a need for improvement, particularly in reducing the working temperature and enhancing selectivity and long-term stability (8). Gas sensors consisting of only MOS often encounter issues with poor selectivity, primarily stemming from the uniform sensing mechanism occurring predominantly at the surface and their requirement for relatively high operating temperatures (9).

In recent years, there has been extensive research was conducted on composite materials to address this restrictions. Notably, composite materials enhance electrical properties(10). As one of the most studied p-type conducting polymers, PANI has garnered significant interest as a promising component in multifunctional composite materials due to its intrinsic electrical conductivity, environmental stability, and facile synthesis under ambient conditions (11). A P–N heterojunction is formed upon the combination with MOS, leading to an improved gas-sensing performance (12). The PANI and ZnO thin films (13) and nonwoven composite materials (14) have been investigated thoroughly. Yet, limited research exists on the use of PANI and ZnO fiber gas sensors. However, because of its rigid molecular structure and limited solubility, pure PANI solution cannot be electrospun directly. In order to increase the viscosity of the precursor solution and enable electrospinning, the host polymer, typically insulating polymers devoid of gas sensing activity, must be added to the mixture. The specific surface area of the PANI composite can be significantly increased by successfully electrospinning the PANI solution into fibers with the addition of the host polymer (15).

As a host polymer, polyacrylonitrile (PAN) was used, since it offers a flexible and porous fiber matrix, and its use as a structural backbone in electrospun fibers immobilizes ZnO particles while providing mechanical support (16). However, the increase in the specific surface area of the PANI electrospun fibers has not increased the gas sensitivity effectively. This is because a large number of PANI molecules were embedded in the inner layer of the

fibre and were unable to interact with the analyte, since the majority of the fibre surface was occupied by the host polymer, which had a significantly higher content than PANI in the precursor solution (15). Thus, this study used the strategy of coating electrospun ZnO-PAN polymer with PANI, to increase its number of active sites.

No extensive research has been conducted on the use of a PAN/ZnO/PANI composite fiber for NH gas sensing applications until this point. In this study, a novel gas sensing material was developed by integrating sol-gel synthesized ZnO nanoparticles into a polyacrylonitrile (PAN), followed by electrospinning to form composite nanofibers and polyaniline (PANI) matrix coating. This unique combination of high surface area, electrical conductivity, and chemical reactivity offers enhanced NH detection capabilities at room temperature. The synergy between the semiconducting ZnO nanoparticles and the conductive PANI phase enables efficient charge transfer and selective gas interaction, resulting in a versatile, flexible, and high-performance sensing platform suitable for practical ammonia detection applications.

2 Methodology

To fabricate ZnO nanoparticles, the sol-gel technique (17) was used. Specifically, 20 mL of ethanol and 6 g of $Zn(CH_3CO_2)_2$ were mixed and stirred at 60 ℃ on a hot plate for 2 h. The mixture was annealed for 2 h in an air atmosphere at 600 ℃ to obtain ZnO. In the following step, the electrospinning technique was used to fabricate ZnO-loaded composite fibers. 35 wt% PAN solution was made by dissolving PAN powder in DMF solution at 45 ℃ for 2 h while stirring continuously. Next, to produce a spinning solution, ZnO dispersion was added to the polymer and stirred for 2 h. Next, the prepared spinning solution was injected into a 10 mL plastic syringe. The electrospinning process was conducted using optimized parameters (18) as follows: applied voltage was 23 kV, the distance between the collector and the tip of the needle is 17 cm, and the flow rate was 1 mL/h. Fibers were then dried for 5 h at 60 ∘C. The PANI coating was polymerized in situ. 0.1M of APS solution was added dropwise into the 0.1M aniline solution (in the ratio of 1:1) together with immersed electrospun fibers in the HCl acid environment of pH 4 and stirred for 7 h in an ice bath.

To determine the phase and crystallinity of the obtained powders, X-ray diffraction analysis (XRD, Rigaku MiniFlex 600 X-ray diffractometer, Japan) with a Cu K source (= 1.54 Å) radiation was used. The diffraction patterns were set from 10∘ to 80∘ with an increment of 0.01∘/5 s. Scanning electron microscopy (SEM, EDX ZEISS Crossbeam 540, Germany) was used to examine the morphology and microstructure of the samples, as well as energy-dispersive X-ray spectrometry (EDS) to determine the elements in the composite. The SEM samples were previously coated with gold using an automatic sputter coater (Q150T, Japan). Investigation of internal microstructures was conducted via Transmission electron microscope (TEM) images using JEM-1400 Plus (JEOL, Japan) at 120 kV accelerating voltage. Various functional groups and chemical compositions of the samples were analyzed via Fourier transform infrared spectroscopy (FTIR, Thermo Fisher Scientific Nicolet iS10 FT-IR Spectrometer, USA). The newly obtained sample band-gap was analyzed using Ultraviolet-visible spectrophotometer for solid state samples (Shimadzu UV-2600i, Japan).

3 Results and Discussions

XRD analysis was used to examine the synthesised ZnO's structural phase purity. Figure 1 displays the XRD pattern, which has several diffraction peaks between 25-80°. The peaks at 31.7°, 34.48°, 36.25°, 47.51°, 56.56°, 62.91°, 66.38°, 67.91°, 69.18°, and 77.04°are indexed as the (100), (002), (101), (102), (110), (103), (200), (112), (201), and (202), confirming the lattice planes of ZnO and the absence of impurities. The wurtzite structure of the obtained ZnO is compatible with JCPDS file No. 01–080–3004. ZnO has good crystallinity, as evidenced by the narrower breadth and increased intensity of the diffraction peaks (19). The performance of the sensor is positively impacted by ZnO nanoparticles' crystallinity. Generally, more crystallinity results in better electrical conductivity, which raises the sensitivity and reaction time of the sensor. Additionally, crystalline ZnO offers additional gas adsorption active sites, enhancing the sensor's ammonia detection capabilities (19). In sensor applications, higher crystalline often leads to increased structural stability, which lowers drift over time and enhances long-term dependability.

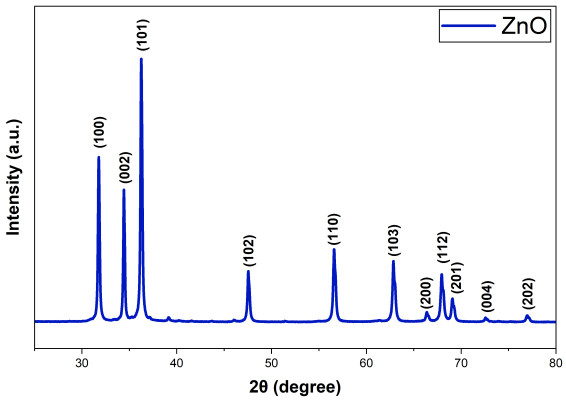
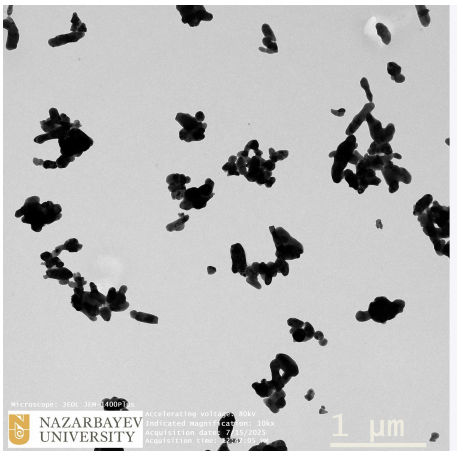
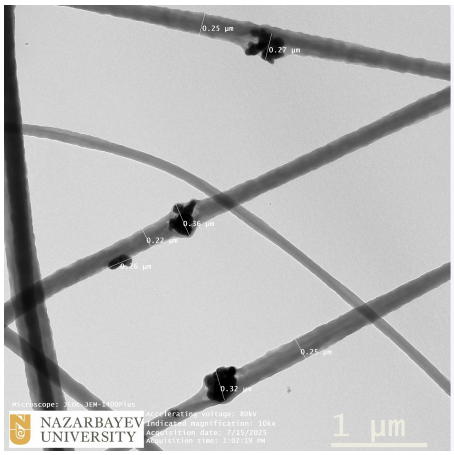


Figure 1: XRD graph of synthesized ZnO NPs.

The formation and dispersion of ZnO NPs were studied using Transmission Electron Microscopy (TEM), as shown in Fig. 2a. NPs had irregular morphologies with partial agglomeration and sizes ranging approximately from 250 to 400 nm. While individual particles could be distinguished, clustering was evident. The thin coating of PANI was noticeable with fiber diameters ranging from 200 to 250 nm in Fig. 2b. The morphology of the observed samples was characterized using Scanning Electron Microscopy (SEM), depicted in Fig. 3. The fibers exhibited a uniform structure. The fibrous network showed smooth surfaces and intersecting arrangements, providing potential for enhanced porosity and surface area. Localized clusters of ZnO NPs were not uniformly distributed along the fiber length.



(a) ZnO NPs



(b) PANI-coated ZnO (20% w/w) - PAN Composite Fibers.

Figure 2: TEM Images

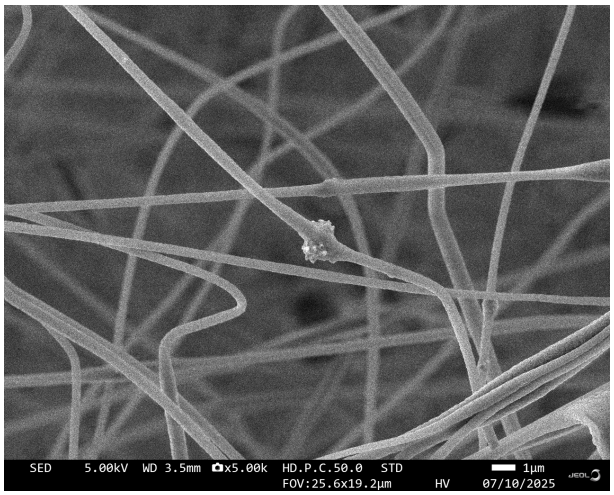
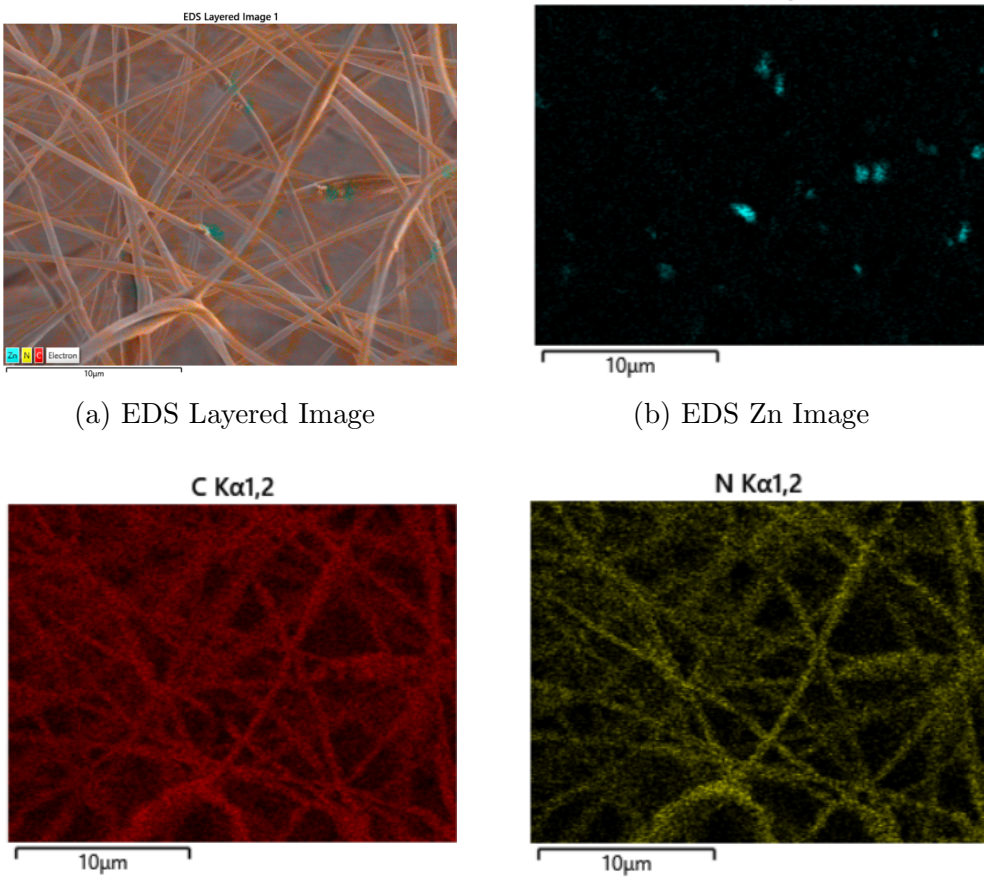


Figure 3: SEM image of PANI-coated ZnO (20% w/w) - PAN Composite Fibers.

The Energy Dispersion Spectroscopy (EDS) was applied to the distribution of the elements Figure.4a. In Figure.4b Zn showed the location of the inorganic doping, and the C and N elements were attributed to the polymer and the coating. NPs were located throughout the fibers in aggregates. The NPs had the shape of beads collected in a thread, and they were in close contact or at distances of 600–900 nm in some areas. The fibers were mainly built of polymer, and the actual amount of ZnO in the fibers appeared to be lower. It could be explained by the precipitation of ZnO agglomerated in the syringe.



(a) EDS Layered Image (b) EDS Zn Image

(c) EDS C Image (d) EDS N Image

Figure 4: EDS Mapping

FTIR spectrum of the developed PANI-ZnO-PAN fibers exhibited the expected peaks with the characteristic peaks, shown in fig. 5. The 680 cm^1 peak was attributed to out-of-plane bending vibrations of C-H bonds in substituted benzenes (20), while the 1042 cm^1 peak is commonly associated with in-plane bending vibrations of C-H bonds in aromatic rings (20). Several peaks were linked to the PANI structure. 1247 cm^1 stretching vibrations were corresponded to C-N in the benzenoid and quinoid units, 1431 cm^1 was linked to C=C in the benzenoid units, and the 1550 cm^1 peak indicated C=C stretching in the quinoid units (21). Similar observations could be made about the peaks related to PAN structure, since the absorption band at 2088 cm^1 corresponds to the stretching vibration of CN groups in the polyacrylonitrile backbone. As indicated in the figure, the peak at 560 cm^1 was related to the Zn-O bond (22). No broad vibrations in the range of 3700-3900 cm^1 mean that there was limited exposure to moisture and negligible oxidation, since this range is associated with O-H stretching. Therefore, FTIR analysis confirmed the presence of ZnO NPs in the PAN fiber matrix and their interaction with PANI.

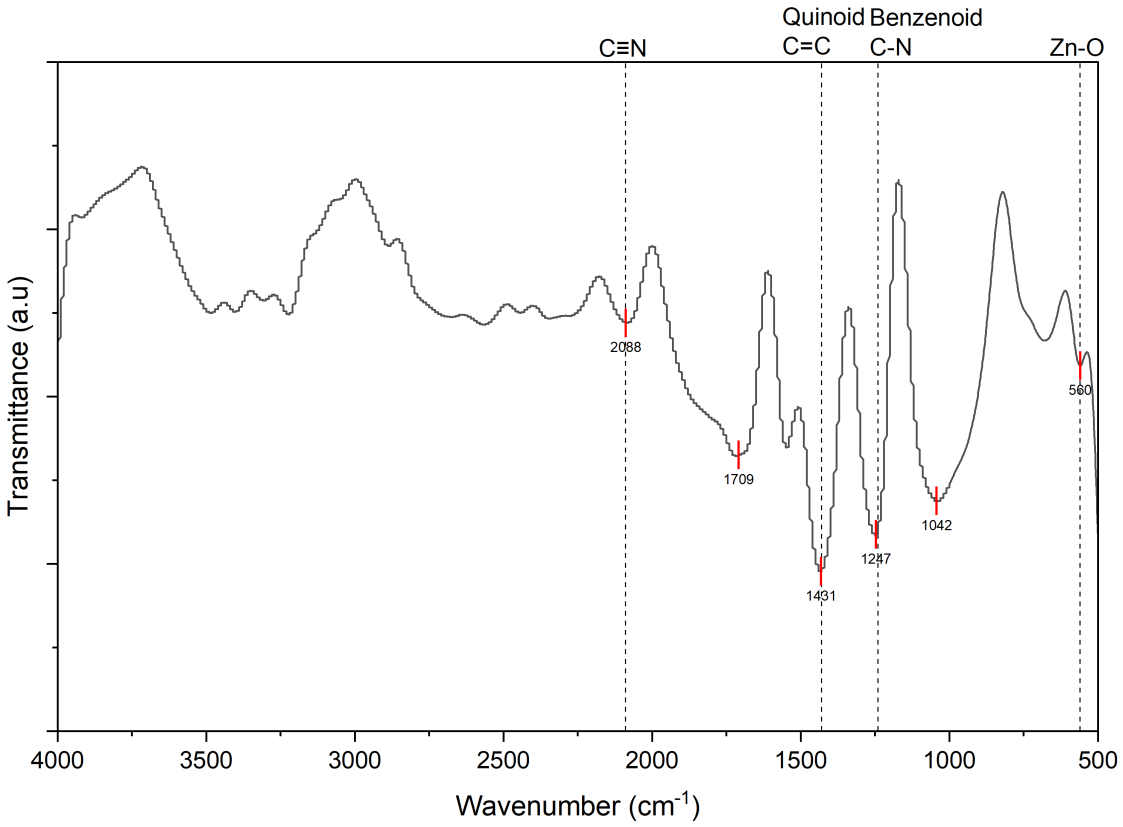


Figure 5: FTIR Spectrum of PANI-coated ZnO (20% w/w) - PAN Composite Fibers

Wavenumber (cm^{-1})	Functionality
560	Zn-O stretching
595	C-N-C bonding of aromatic ring
1042	C-H out of plane bonding in benzoid ring
1170	Spectra of PANI-ZnO
1247	The quinoid of PANI
1566	C=C stretching of quinoid ring
1581	C=N stretching of quinoid ring
3230-3480	Hydrogen bonding between H-N (PANI) and oxygen of ZnO
3648	N-H stretching

Table 1: Characteristic absorption peaks obtained from FTIR spectrum of PANI-coated ZnO (20% w/w) - PAN Composite Fibers.

UV-Vis Diffuse Reflectance Spectroscopy (DRS) The band gap energy can be calculated by using the following Tauc equation:

$$(\alpha h\nu)^n = A(h\nu - E_g) \tag{23}$$

where α, h, and ν are the absorption coefficient, Planck's constant, and light frequency, respectively, while A is a constant and the value of n depends on whether the transition is direct ($n = \frac{1}{2}$) or indirect ($n = 2$).

According to Fig. 6, the value of the gap energy of PANI/ZnO nanocomposite was obtained by drawing a straight line on the slope of the curve until it cuts the x axis. The intersection of a straight line on the slope of the curve with the x-axis shows the value of the bandgap energy. The band gap yield obtained in PANI/ZnO (20% w/w) nanocomposites was 2.037 eV. The connection between PANI and ZnO is confirmed by the reduced bandgap of synthesised composite photocatalysts (3.37 eV) when compared to pure ZnO (24). Because PANI was in its conductive form and ZnO dissolution was impeded, the in situ synthesis was successful.

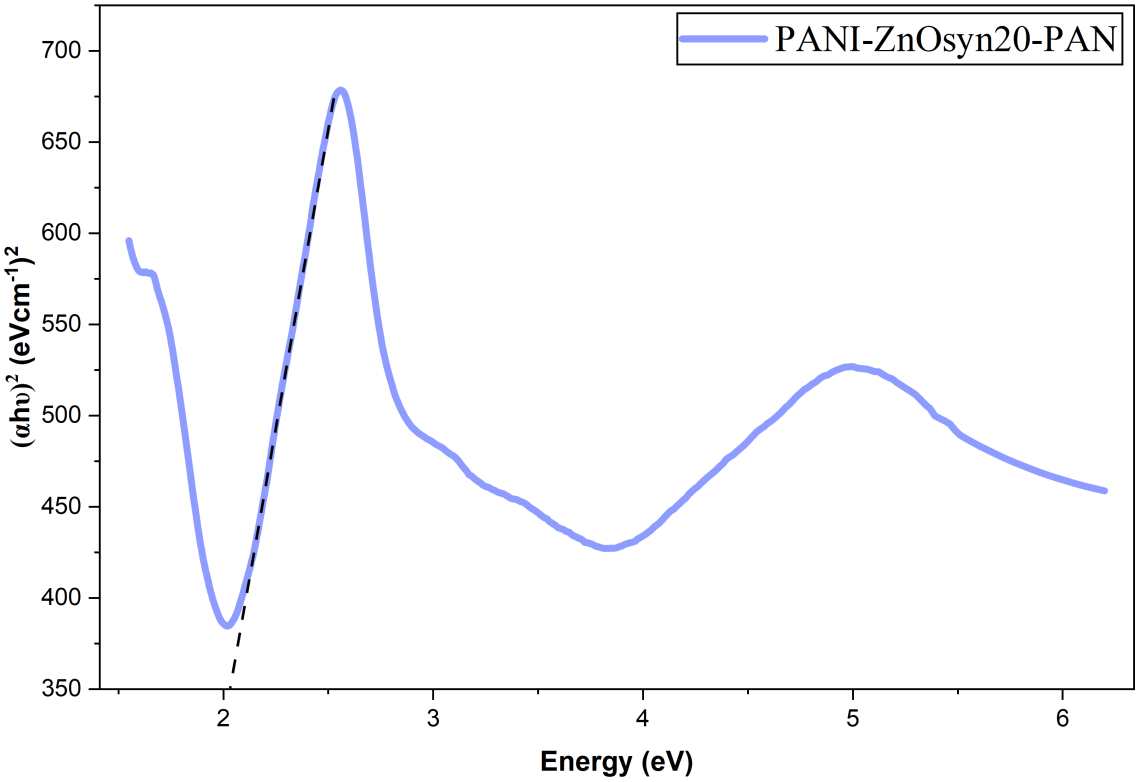


Figure 6: UV-Vis Spectroscopy image of PANI-coated ZnO (20% w/w) PAN Composite Fibers using the Tauc Plot method.

4 Further Research

The ambient room temperature will be about 23 °C. Relative humidity (RH) will be varied between 10-80% (25). The sensing response of the generated sensors was calculated by comparing the change in electrical resistance upon exposure to different gases to the baseline established in the air atmosphere. The formula was used to calculate the sensing

response of the produced sensors:

$$S = \frac{\Delta R}{R_g} = \frac{R_a - R_g}{R_g} \tag{11}$$

where Ra and Rg represent the resistance of the sensor in air and target gas medium.

There are several other metrics for gas sensor performance evaluation. Time to reach 90% of full signal after gas exposure (Response time). Time to return to 90% of baseline after gas is removed (Recovery time). Lowest concentration that shows a measurable response (Limit of Detection (LOD)) (17).

There's noticeable agglomeration and non-uniformity of ZnO NPs. To combat this issue, it's desirable to improve fiber structure and ZnO distribution to maximize active surface area. To achieve this goal, there's a proposal to vary electrospinning parameters systematically (voltage, flow rate, PAN concentration). Next, analysis of resulting fiber diameter, porosity, and ZnO dispersion via SEM/TEM is important, using response surface methodology (RSM) to find optimal conditions (18).

A sensor that works once but degrades quickly cannot be used practically. Long-term stability is essential for commercial viability. To assess whether the sensor maintains stable performance over time and under environmental stresses (e.g., air exposure, cycles, temperature shifts), it's desirable to conduct cycle, environmental and mechanical stress tests (4).

5 Conclusion

In this study, PANI–ZnO–PAN composite fibers were successfully synthesized using a combination of sol–gel, electrospinning, and in-situ polymerization techniques. Structural and morphological analyses confirmed the successful incorporation of ZnO nanoparticles within the PAN fiber matrix and the uniform coating of PANI on the fiber surfaces. FTIR spectra verified the presence of characteristic functional groups associated with PANI, PAN, and ZnO, while TEM and SEM imaging revealed the composite's porous and interconnected fibrous network. The synergy between the semiconducting ZnO nanoparticles and the conductive PANI phase offers a promising route for room-temperature ammonia gas sensing with potentially enhanced sensitivity, selectivity, and stability. Although gas-sensing measurements and real-world testing were not performed due to time constraints, the material characterization suggests that this composite structure holds significant potential for future gas sensor development.

6 Acknowledgments

The author wishes to express sincere gratitude to Aida Barlybaeva, PhD Candidate, Nazarbayev University, for her invaluable assistance in demonstrating experimental procedures, sharing datasets, and reviewing the manuscript. The author also thanks Almagul Mentbayeva, Nazarbayev University for their guidance throughout the project. This research experience was made possible through the support of the Research Orda Kazakhstan.

References

(1) Kwak, D.; Lei, Y.; Maric, R. Ammonia Gas Sensors: A Comprehensive Review. *Talanta* **2019**, 204, 713–730. https://doi.org/10.1016/j.talanta.2019.06.034

(2) Zhu, C.; Zhou, T.; Xia, H.; Zhang, T. Flexible Room-Temperature Ammonia Gas Sensors Based on PANI-MWCNTs/PDMS Film for Breathing Analysis and Food Safety. *Nanomaterials* **2023**, 13(7). https://doi.org/10.3390/nano13071158

(3) Majhi, S. M.; Mirzaei, A.; Kim, H. W.; Kim, S. S.; Kim, T. W. Recent Advances in Energy-Saving Chemiresistive Gas Sensors: A Review. *Nano Energy* **2021**, 79. https://doi.org/10.1016/j.nanoen.2020.105369

(4) Indarit, N.; Kim, Y.-H.; Petchsang, N.; Jaisutti, R. Highly Sensitive Polyaniline-Coated Fiber Gas Sensors for Real-Time Monitoring of Ammonia Gas. *RSC Advances* **2019**, 9(46). https://doi.org/10.1039/C9RA04005F

(5) Darwish, M. A.; Abd-Elaziem, W.; Elsheikh, A.; Zayed, A. A. Advancements in Nanomaterials for Nanosensors: A Comprehensive Review. *Nanoscale Advances* **2024**, 6(16), 4015–4046. https://doi.org/10.1039/D4NA00214H

(6) Alenezi, M. R.; Henley, S. J.; Emerson, N. G.; Silva, S. R. P. From 1D and 2D ZnO Nanostructures to 3D Hierarchical Structures with Enhanced Gas Sensing Properties. *Nanoscale* **2014**, 6(1), 235–247. https://doi.org/10.1039/C3NR04519F

(7) Bhati, V. S.; Hojamberdiev, M.; Kumar, M. Enhanced Sensing Performance of ZnO Nanostructures-Based Gas Sensors: A Review. *Energy Reports* **2020**, 6, 46–62. https://doi.org/10.1016/j.egyr.2019.08.070

(8) Wang, Y.; Ma, S.; Wang, L.; Jiao, Z. A Novel Highly Selective and Sensitive NH_3 Gas Sensor Based on Monolayer Hf_2CO_2. *Applied Surface Science* **2019**, 492, 116–124. https://doi.org/10.1016/j.apsusc.2019.06.212

(9) Zhang, J.; Liu, X.; Neri, G.; Pinna, N. Nanostructured Materials for Room-Temperature Gas Sensors. *Advanced Materials* **2015**, 28(5), 795–831. https://doi.org/10.1002/adma.201503825

(10) Preethichandra, D. M. G.; Gholami, M. D.; Izake, E. L.; O'Mullane, A. P.; Sonar, P. Conducting Polymer Based Ammonia and Hydrogen Sulfide Chemical Sensors and Their Suitability for Detecting Food Spoilage. *Advanced Materials Technologies* **2022**, 8(4), 2200841. https://doi.org/10.1002/admt.202200841

(11) Hsueh, T.-J.; Ding, R.-Y. A Room Temperature ZnO-NPs/MEMS Ammonia Gas Sensor. *Nanomaterials* **2022**, 12(19). https://doi.org/10.3390/nano12193287

(12) Foronda, J. R. F.; Aryaswara, L. G.; Santos, G. N. C.; Raghu, S. N. V.; Muflikhun, M. A. Broad-Class Volatile Organic Compounds Detection via Polyaniline/Zinc Oxide Composite Materials as Gas Sensor Application. *Heliyon* **2023**, 9(2). https://doi.org/10.1016/j.heliyon.2023.e13544

(13) Dhanve, S. P.; Gutte, Y. P.; Birajdar, C. T. Investigating the Physicochemical and Optical Properties of PANI and PANI-ZnO Thin Films for an Efficient Ammonia Sensor at Ambient Conditions. *Chemical Papers* **2025**, 79(4), 2121–2130. https://doi.org/10.1007/s11696-025-03911-1

(14) Guan, Y.; Wang, C.; Yu, H.; Zou, Z.; Zhou, Y.; Cao, G.; Yao, J. Flexible ZnO/PANI/Nonwoven Nanocomposite Based High-Sensitive NH_3 Gas Sensor via Vapor Phase Polymerization Method. *Materials Science for Energy Technologies* **2020**, 3, 862–867. https://doi.org/10.1016/j.mset.2020.10.011

(15) Qu, C.; Zhao, P.; Wu, C.; Zhuang, Y.; Liu, J.; Li, W.; Liu, Z.; Liu, J. Electrospun PAN/PANI Fiber Film with Abundant Active Sites for Ultrasensitive Trimethylamine Detection. *Sensors and Actuators B: Chemical* **2021**, 338. https://doi.org/10.1016/j.snb.2021.129822

(16) Iatsunskyi, I.; Vasylenko, A.; Viter, R.; Kempiński, M.; Nowaczyk, G.; Jurga, S.; Bechelany, M. Tailoring of the Electronic Properties of ZnO-Polyacrylonitrile Nanofibers: Experiment and Theory. *Applied Surface Science* **2017**, 411, 494–501. https://doi.org/10.1016/j.apsusc.2017.03.111

(17) Rakhmanova, A.; Soltabayev, B.; Ajjaq, A.; Khan, N.; Kalybekkyzy, S.; Acar, S.; Mentbayeva, A. Nanofibrous ZnO-Loaded PVA/PEDOT:PSS for Selective and Enhanced Ammonia Detection. *Sensors and Actuators B: Chemical* **2024**, 426. https://doi.org/10.1016/j.snb.2024.137022

(18) Rakhmanova, A.; Kalybekkyzy, S.; Soltabayev, B.; Bissenbay, A.; Kassenova, N.; Bakenov, Z.; Mentbayeva, A. Application of Response Surface Methodology for Optimization of Nanosized Zinc Oxide Synthesis Conditions by Electrospinning Technique. *Nanomaterials* **2022**, 12(10). https://doi.org/10.3390/nano12101733

(19) Mendes, C. R.; Dilarri, G.; Forsan, C. F.; Sapata, V. M. R.; Lopes, P. R. M.; de Moraes, P. B.; Montagnolli, R. N.; Ferreira, H.; Bidoia, E. D. Antibacterial Action and Target Mechanisms of Zinc Oxide Nanoparticles against Bacterial Pathogens. *Scientific Reports* **2022**, 12(1). https://doi.org/10.1016/j.fpsl.2023.101167

(20) Alamgeer; Tahir, M.; Sarker, M. R.; Ali, S.; Ibraheem; Hussian, S.; Ali, S.; Imran Khan, M.; Khan, D. N.; Ali, R.; Mohd Said, S. Polyaniline/ZnO Hybrid Nanocomposite: Morphology, Spectroscopy and Optimization of ZnO Concentration for Photovoltaic Applications. *Polymers* **2023**, 15(2), 363. https://doi.org/10.3390/polym15020363

(21) Ibrahim, K. A. Synthesis and Characterization of Polyaniline and Poly(Aniline-Co-o-Nitroaniline) Using Vibrational Spectroscopy. *Arabian Journal of Chemistry* **2014**, 10. https://doi.org/10.1016/j.pnsc.2012.07.002

(22) Noei, H.; Qiu, H.; Wang, Y.; Löffler, E.; Wöll, C.; Muhler, M. The Identification of Hydroxyl Groups on ZnO Nanoparticles by Infrared Spectroscopy. *Physical Chemistry Chemical Physics* **2008**, 10(47). https://doi.org/10.1039/B811029H

(23) Gilja, V.; Vrban, I.; Mandić, V.; Žic, M.; Hrnjak-Murgić, Z. Preparation of a PANI/ZnO Composite for Efficient Photocatalytic Degradation of Acid Blue. *Polymers* **2018**, 10(9). https://doi.org/10.3390/polym10090940

(24) Andreas, R.; Lesbani, A.; Akhmad Yusuf, F. The Characteristics of Nanocomposites Polyaniline (PANI)/ZnO. *IOP Conference Series: Materials Science and Engineering* **2019**, 509. https://doi.org/10.1088/1757-899X/509/1/012126

(25) Alaghmandfard, A.; Fardindoost, S.; Hoorfar, M. Effect of Au Nanoparticles on Mitigating the Negative Impacts of Humidity on ZnO Gas Sensors to Detect Triethylamine at Room Temperature. *Applied Surface Science Advances* **2024**, 22, 100623. https://doi.org/10.1016/j.apsadv.2024.100623

References